Article

Management Transition to the Great Lakes Nearshore: Insights from Hydrodynamic Modeling

Chenfu Huang [1], Anika Kuczynski [1,2] , Martin T. Auer [1], David M. O'Donnell [3] and Pengfei Xue [1,*]

[1] Department of Civil and Environmental Engineering and Great Lakes Research Center Michigan Technological University, Houghton, MI 49931, USA; chenfuh@mtu.edu (C.H.); anika.kuczynski@niwa.co.nz (A.K.); mtauer@mtu.edu (M.T.A.)

[2] Presently, National Institute of Water and Atmospheric Research, Christchurch 8011, New Zealand

[3] Upstate Freshwater Institute, Syracuse, New York, NY 13206, USA; daveod@ourlake.org

[*] Correspondence: pexue@mtu.edu; Tel.: +1-906-487-1837

check for updates

Abstract: The emerging shift in Great Lakes management from offshore to nearshore waters will require attention to complexities of coastal hydrodynamics and biogeochemical transformations. Emphasizing hydrodynamics, this work resolves transport processes in quantifying discharge plume and pollutant of concern (POC) footprint dimensions, the latter being the portion of the plume where water quality standards are not met. A generic approach, isolated from pollutant-specific biokinetics, provides first-approximation estimates of the footprint area. A high-resolution, linked hydrodynamic-tracer model is applied at a site in the Greater Toronto Area on Lake Ontario. Model results agree with observed meteorological and hydrodynamic conditions and satisfactorily simulate plume dimensions. Footprints are examined in the context of guidelines for regulatory mixing zone size and attendant loss of beneficial use. We demonstrate that the ratio of the water quality standard to the POC concentration at discharge is a key determinant of footprint dimensions. Footprint size for traditional pollutants (ammonia, total phosphorus) meets regulatory guidelines; however, that for soluble reactive phosphorus, a presently unattended pollutant, is ~1–2 orders of magnitude larger. This suggests that it may be necessary to upgrade treatment technologies to maintain consistency with regulatory guidelines and mitigate manifestations of the eutrophication-related soluble reactive phosphorus POC.

Keywords: hydrodynamics; plume; footprint; Great Lakes; pollutant of concern

1. Introduction

Located at the watershed–waterbody interface, coastal margins are both the primary standard for stakeholder perception of water quality and a bellwether of future conflict in ecosystem services. The Laurentian Great Lakes include 9783 miles of coastal margin in the United States (US) and Canada, and collectively have long been referred to as "the inland seas" [1]. North America's *inland seas* are likened to ocean systems, as coastal dynamics in both are driven by similar physical processes (e.g., coastal jets [2–4]). Unlike the coastal oceans, however, the Great Lakes are closed systems where the influence of hydrodynamic phenomena on ecosystem function is magnified [4]. For example, discharges to nearshore waters may be entrained by coastal jets, extending the region of influence along the broader coastal zone beyond the point of entry and into the larger lake [4–6]. Similarities between the coastal margin of marine and large lake systems are such that similar challenges are faced [7] and common hydrodynamic modeling platforms are often utilized in simulating mass transport (e.g., Princeton Ocean Model (POM) [8], Finite Volume Community Ocean Model (FVCOM) [9,10], Estuary

and Lake Computer Model (ELCOM) [11]). In regulatory applications, engineering design guidance for ocean outfalls and offshore discharges to freshwaters share a common manual [12]. As a result of these similarities, contributions to the body of knowledge on physical processes in large lakes merit a place in the coastal ocean literature (historically [3] and more recently [13,14]).

1.1. Science, Engineering, and Management Context

Management of pollutants of concern (POCs) in the nearshore calls for an approach that is radically different from that applied to open lakes and offshore waters. The open lake is often conceptualized as a completely mixed system where, upon input, individual loads are mixed instantaneously across the entire water body, resulting in only a modest increase in lakewide pollutant concentration and attendant impact (Figure 1a). However, this conceptualization translates poorly to the nearshore. Coastal zone management recognizes the system as being incompletely mixed as tributary and point source inputs are received at locations proximate to the land–water boundary. These inputs are retained in the nearshore for extended periods, potentially becoming juxtaposed with receptors (e.g., beaches, algal habitat, water intakes), while undergoing dilution and biokinetic transformation prior to transport to the open lake (Figure 1b). This conceptualization of the nearshore highlights the importance of nutrient loading reductions and separation of nutrient-rich point source effluent plumes from algal habitat in ecosystem management, with common approaches including advanced point source treatment and extension of offshore discharges (see Reference [15]).
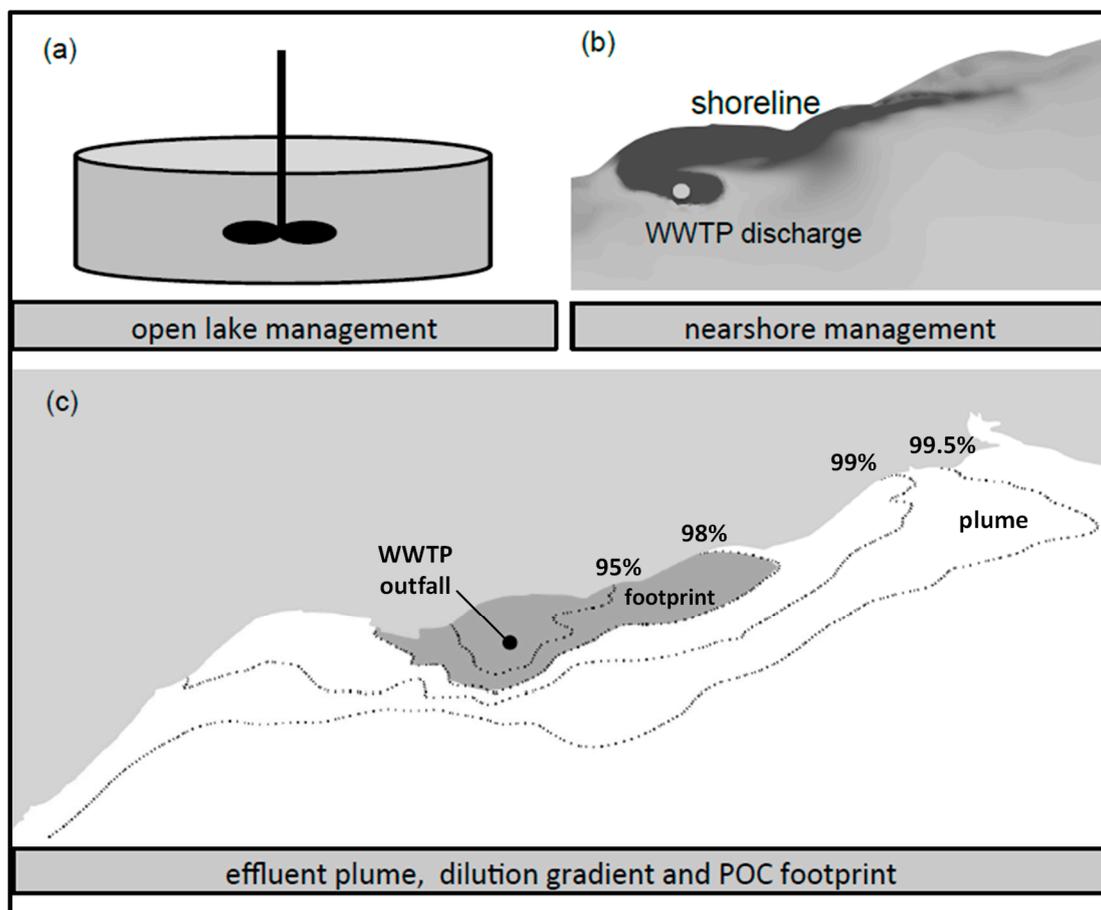

Figure 1. Conceptualization of water quality management in (**a**) an open lake and (**b**) a nearshore context, and (**c**) an effluent plume, over which a dilution gradient (dashed lines) is manifested, as well as the footprint for a pollutant of concern (gray shading). The extent of the plume is set arbitrarily at the 99.5% dilution isopleth and represents the confluence of water containing effluent and the unimpacted boundary condition. The extent of the footprint is set at the 98% dilution isopleth for this example.

Point source engineering design for achieving the required separation between nutrient-rich wastewater effluent plumes (Figure 1b,c) and receptors begins with the definition of discharge plume dimensions. The plume boundary marks the location at which constituent concentrations in plume waters approach those of ambient waters, illustrated in Figure 1c as the 99.5% dilution isopleth. The footprint is located within the plume and represents the region in which the POC concentration exceeds the water quality standard (illustrated in Figure 1c as the 98% dilution isopleth). In regulatory applications, a mixing zone is defined as a region where compliance with water quality standards is not required [16]. However, regulatory guidelines state that mixing zones are to be kept as small as possible, not interfere with beneficial uses, and not be used as an alternative to reasonable and practicable treatment [16]. Where a POC footprint conforms to these guidelines, regulatory objectives are met, water quality management goals are realized, and the terms footprint and mixing zone may be considered synonymous. Where guidelines are not met, the discharge must be moved further offshore (enhancing separation from receptors) or additional treatment (e.g., reducing discharge effluent concentration) is required. The focus of this work is to characterize plume and footprint dimensions for tributary and point source inputs and better understand their impacts on coastal zone management.

1.2. Study Site

The western shoreline of Lake Ontario is characterized as "an almost unbroken urban landscape" extending from the mouth of the Niagara River, across the Greater Toronto Area (GTA), to Oshawa, Ontario (ON) [17] (Figure 2) and is today home to a population approaching seven million. Eastward along the north shore, land use is dominated by agriculture with some forest cover. A gradient in phosphorus enrichment and attendant water quality parallels the gradient in urbanization [18–21]. In the lesser developed region to the east of the GTA, that gradient is overlain by a mosaic of discharges from generally small tributaries and wastewater treatment plants [21]. While consensus was built regarding the significance of effluent plumes, a critical knowledge gap remains in establishing plume dimensions (i.e., longshore and offshore extent) and their residence time in the nearshore.

The study site is located along a 25-km stretch of the Lake Ontario nearshore from Pickering to Whitby, ON, centered on Ajax, ON and extending offshore for a distance of ~3 km (4.5 km at two stations; Figure 2). Although positioned near the eastern boundary of the GTA, the study site remains highly developed. Maximum depths range from 20 to 35 m, the approximate point of separation for nearshore and offshore waters in Lake Ontario [22] (see also References [5,6]). Three tributaries (the Rouge River, and Duffins and Carruthers Creeks), three wastewater treatment plants (WWTPs; Highland Creek, Duffin Creek, and Corbett Creek), and the Pickering Nuclear Generating Station (PNGS; cooling water intake and discharge) are located within the study site (Figure 2; Figure 3; Table 1). Based on total phosphorus (TP) load [19], the Duffin Creek, Highland Creek, and Corbett Creek WWTPs are, respectively, the second, seventh, and ninth largest of the 38 plants discharging to the Canadian waters of Lake Ontario [19]. The Pickering Nuclear Generating Station withdrawal and return represents use for once-through cooling water. While this intake and discharge impacts local flow conditions, it has no impact on water quality constituents.
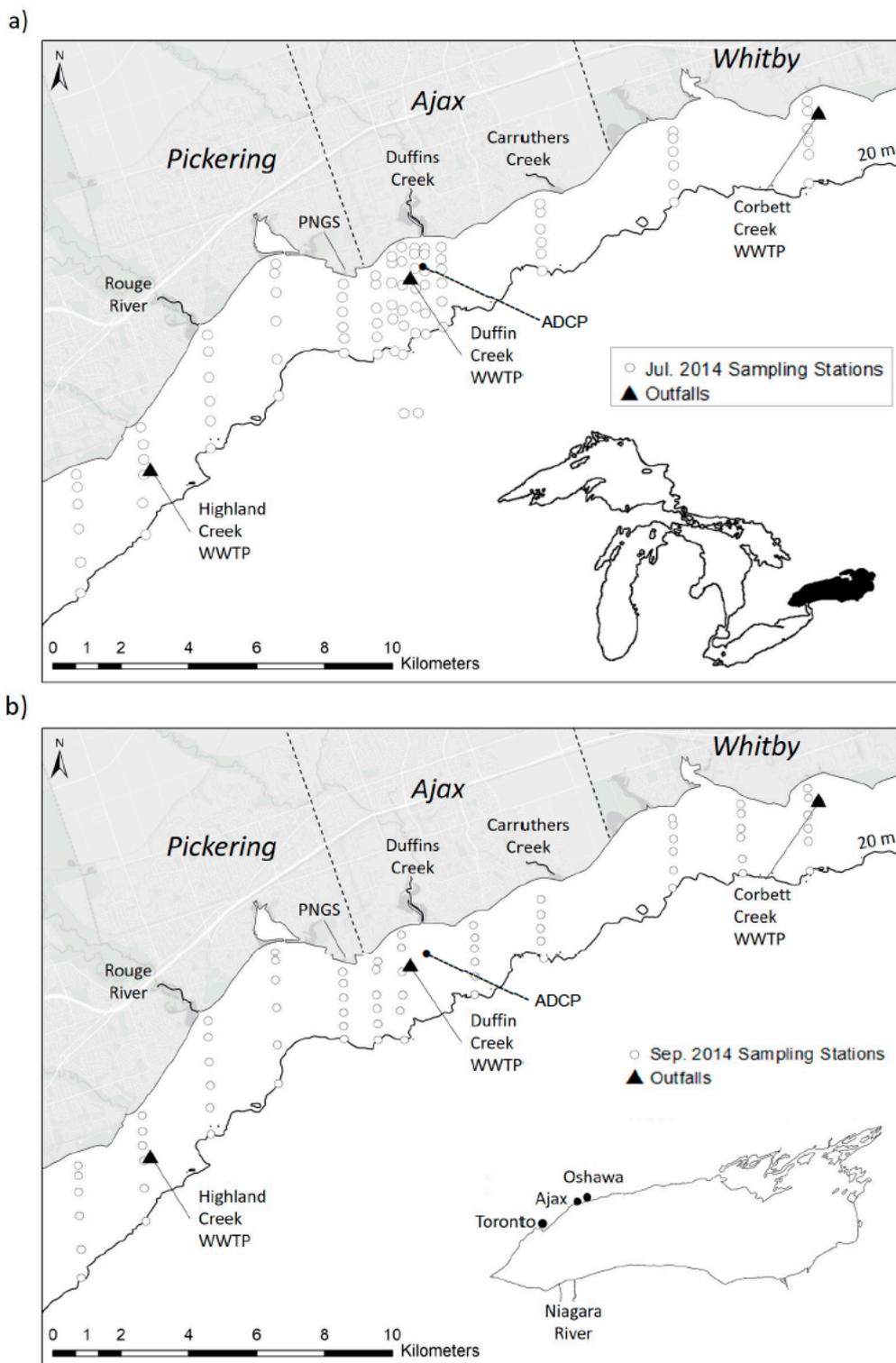
Figure 2. Lake Ontario study site with locations of point source and tributary discharges and sampling stations for July and September 2014 monitoring. Insets in panels (**a**) and (**b**) locate Lake Ontario on the Great Lakes and geographical locations cited in text, respectively.

Management of POCs in the Pickering → Ajax → Whitby nearshore is a source of public concern [23]. For example, this region experiences nuisance growth of the attached, filamentous, green alga *Cladophora* with episodic beach fouling leading to loss of beneficial uses [24]. Nuisance growth is stimulated by sources of soluble reactive phosphorus (SRP), the freely and fully available form of

the nutrient [24,25]. The western portion of our site was the subject of field and hydrodynamic water quality modeling studies in 2007 and 2008 [11]. The authors reported that the outfall from the Duffin Creek WWTP was responsible for elevated SRP levels noted in both field monitoring and modeling results. It was concluded that, if model-predicted episodic elevations in SRP (some not observed in monitoring data) were real, they could have a significant stimulatory impact on *Cladophora*. We believe that the episodic events were caused by incursions of SRP-rich WWTP effluent across their study area, reflecting the highly dynamic nature of the nearshore environment. Thus, our interest is in more fully capturing plume dimensions and characterizing pollutant of concern footprints for the tributary and point source discharges to the Pickering → Ajax → Whitby nearshore. This location was also the focus of studies quantifying phosphorus loads [26] and characterizing the *Cladophora*-phosphorus dynamic through monitoring [11,21,27–31].

Table 1. Tributary and point source discharges included in the study. Tributary flows are summer (May–September) averages, while those for WWTPs are annual averages for 2014. Data sources are footnoted here and described in detail below. Flows provided here facilitate characterization of study site hydrology, while those for specific periods used in model runs are provided in Table 2.

	Flow ($m^3 \cdot s^{-1}$)	Location
Tributaries [1]		
Rouge River	4.31	Scarborough/Pickering, ON
Duffins Creek	2.92	Ajax/Pickering, ON
Carruthers Creek	0.39	Ajax, ON
Point Sources [2]		
Highland Creek WWTP	1.97	Scarborough, ON
Duffin Creek WWTP	3.97	Pickering, ON
Corbett Creek WWTP	0.6	Whitby, ON
Ashbridges Bay WWTP	7.31	Toronto, ON
Pickering Nuclear Generating Station [3]		
PNG A plus PNG B	153.1	Pickering, ON

[1] Environment Canada Water Office (wateroffice.ec.gc.ca); [2] City of Toronto (web.toronto.ca); [3] Ontario Power Generation (www.opg.com).

1.3. Objectives and Approach

More than 15 years ago, Rao et al. [17] warned that the technologies being utilized at wastewater treatment plants discharging to western Lake Ontario were nearing the limits of their design and noted that "the demand for clean water and the need for suitable waste disposal facilities continue to rise at an ever-increasing rate". Since that time, the population estimated at four million by Rao et al. [17] rose to almost seven million and is projected to approach 10 million by 2041 (Statistics Canada, 2017; https://www12.statcan.gc.ca/census-recensement). Yet, the treatment technologies applied across the region (e.g., chemically enhanced secondary treatment for phosphorus) remain those introduced in the 1970s and 1980s. From this, one may posit that a shift in management focus to the Lake Ontario nearshore will reveal a necessity to reassess the impact of POC plumes with respect to regulatory guidelines for coastal waters. We hypothesize that the footprints for previously unattended and emerging POCs may be much larger than traditional POCs and need to be effectively reduced to maintain compliance in a regulatory context.

We test this hypothesis through application of a hydrodynamic model facilitating comparison of effluent and tributary plume and POC footprint dimensions for traditional (e.g., total ammonia nitrogen (TAN) and total phosphorus; see [17]) and a previously unattended POC (soluble reactive phosphorus). Management of POCs requires attention to both mass transport (hydrodynamic processes, unrelated to the type of POC) and biogeochemical (biokinetics, POC-specific) transformations. This work focuses on the first of these, mass transport, with the intent to characterize **POC footprint maxima**. Therefore, the target POC is treated as a conservative substance, an approach appropriate for determination of

discharge plume dimensions and POC *footprint maxima* solely as mediated by mass transport, i.e., in isolation from biokinetic processes.

The hydrodynamic model was developed, and simulations were performed and applied in three steps as follows:

1. Test model performance by comparing output to field measurements to establish the credibility and reliability required to support management decisions;

2. Characterize dynamic plume behavior (e.g., variation in the direction of alongshore movement) as a determinant of plume dimensions;

3. Evaluate POC footprint dimensions for their consistency with mixing zone guidelines for nearshore water quality management.

In testing our hypothesis, we seek to provide guidance for the transition from open lake to nearshore management of previously unattended and/or emerging POCs in the Great Lakes. We believe that our approach and our findings will find application in other large lake and coastal ocean environments exploring the need for next-generation effluent management strategies.

2. Methods

2.1. Field Sampling and Laboratory Methods

Nearshore and coastal waters are highly dynamic, thus posing a challenge with respect to the development of hydrodynamic models. For example, the ability to simulate transport of effluent plumes is highly dependent on the accuracy of modeled current flow. An acoustic Doppler current profiler (ADCP) providing continuous current flow measurements was deployed from July to September 2014 (see Figure 3 for location). ADCP data were processed and analyzed along with meteorological measurements obtained from National Data Buoy Center (NDBC) Buoy 45159 (Figure 3) for validation of hydrodynamic model input forcing and simulation results. In addition, to characterize the spatial variability of effluent plumes and provide ground truth for model calibration and confirmation, we also conducted water quality sampling on 19 July and 9 September 2014. We sampled along 14 transects (86 stations) in July and 12 transects (71 stations) in September, spanning the 25-km breadth of the study site (Figure 3). A YSI 6600 V2-4 multi-parameter water quality sonde and an ISUS V3 sonde were used to obtain surface-to-bottom (1–20 m) profiles of temperature (°C), conductivity (μS/cm), and nitrate (as nitrogen, NO_3-N) at each station.

2.2. Hydrodynamic Modeling Methods

The research described here utilizes the Finite Volume Community Ocean Model (FVCOM), a platform widely applied in estuarine and coastal ocean environments [32–34] and emerging as a commonly used tool for application to the Great Lakes [9,35–38] in both stand-alone hydrodynamic modeling and coupled with a water quality [39] or regional climate model [10,40]. In this section, we describe the methods underlying linkage of a hydrodynamic model with a soluble tracer tracking model. FVCOM, like many other hydrodynamic frameworks used for the Great Lakes (e.g., References [41–45]), is a three-dimensional (3D) free-surface, primitive-equation model that solves the momentum, continuity, temperature, salinity, and density equations, and is closed physically and mathematically using the 2.5 level turbulence submodel [46] for vertical mixing and the Smagorinsky formulation [47] for horizontal diffusion. FVCOM is solved numerically using the finite volume method in the integral form of the primitive equations over an unstructured triangular grid mesh and vertical sigma layers. This approach combines the advantage of an unstructured grid for shoreline fitting and the flexibility of local mesh refinements (similar to finite element methods), as well as numerical efficiency and code simplicity (similar to finite difference methods). These characteristics of FVCOM make it particularly attractive in applications to coastal waters [33], where strong nonlinear interactions occur due to local

geometric complexity and highly variable flow patterns [4,48]. These characteristics make the model well suited for the study of Lake Ontario described here.

Although this study focuses on the Pickering → Ajax → Whitby nearshore (Figure 2), FVCOM is configured to simulate physical dynamics for all of Lake Ontario in a manner similar to that applied by Xue et al. [14], thus providing reliable representation of large-scale background circulation and the role of remote (offshore) forcing in driving nearshore water movement; additionally, this configuration avoids the impact of setting an artificial numerical boundary condition for our target region. The advantage of an unstructured grid is that model resolution varies from 2–4 km (coarse) in the open lake to 50–150 m (fine) in the targeted nearshore, affording a high degree of resolution across the 25-km study site and adequately resolving the geographic complexity and coastal hydrodynamic conditions of that system (Figure 3). The model configuration yields a total of 41,442 grid elements (cells) in the horizontal plane. Vertically, 20 evenly spaced sigma coordinate layers are implemented with a resolution of <1 m in the nearshore region of interest and 5–10 m in the open lake. The bathymetric data used in the hydrodynamic model are derived from a three-arc-second (~90-m cell size), grid-based dataset from https://www.ngdc.noaa.gov/mgg/greatlakes/greatlakes.html. The Great Lakes bathymetric data were compiled by the National Oceanographic and Atmospheric Administration (NOAA) and made available to the public for Great Lakes science.
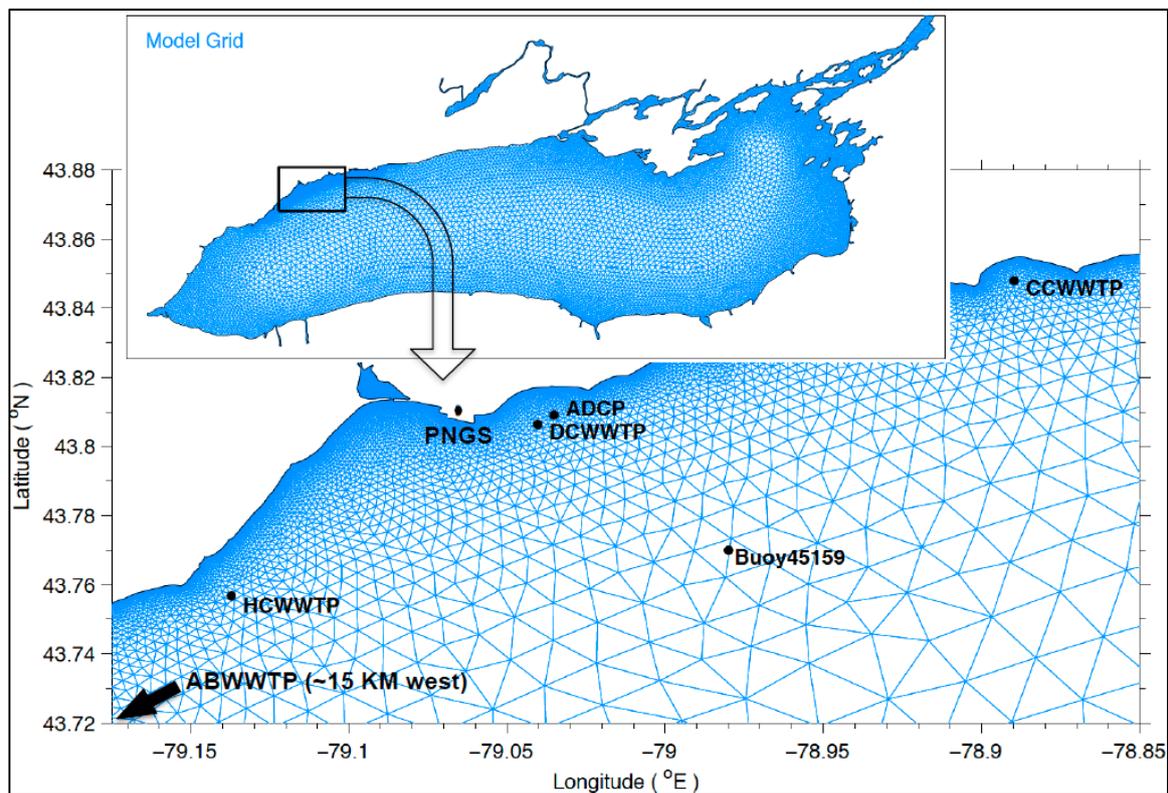

Figure 3. Model mesh for Lake Ontario with additional detail presented for the immediate study area. The locations of wastewater treatment plant (WWTP) outfalls, the acoustic Doppler current profiler (ADCP), the Pickering Nuclear Generating Station (PNGS) and the NDBC buoy are identified.

FVCOM requires input of environmental (meteorological) forcing conditions including downward solar radiation, wind speed and direction, air temperature, atmospheric pressure, relative humidity, and cloud cover. Forcing conditions were obtained as hourly data from the National Centers for Environmental Prediction (NCEP)'s Climate Forecast System Reanalysis (CFSR), a resource that provides meteorological data beginning in 1979, with enhanced horizontal resolution (0.2 degrees, ~20 km) available after 2011. A recent study [37] showed that CFSR reliably represents the wind patterns

and radiation fields required to support robust simulations of circulation patterns and thermal structure in the Great Lakes. The CFSR wind data are also compared to local meteorological measurements from NDBC Buoy 45159 (Figure 3) to ensure accuracy of that input forcing condition at a local scale.

2.3. Soluble Tracer Sub-Model

A soluble tracer-based model is used to simulate the distribution of the effluent plume. The transport and mixing of the plume with a concentration field (C) is calculated using the mass conservation equation as follows:

$$\frac{\partial HC}{\partial t} + \frac{\partial HuC}{\partial x} + \frac{\partial HvC}{\partial y} + \frac{\partial wC}{\partial \sigma} - \frac{1}{H}\frac{\partial}{\partial \sigma}\left(K_h\frac{\partial C}{\partial \sigma}\right) - HF_c = C_{source} - C_{sink},$$ (1)

where H is the total water depth, and u, v, and w are the horizontal and vertical components of the water velocity in the sigma (σ) coordinate system [32]. The σ coordinate transformation is commonly used in the vertical component in order to obtain a smooth representation of irregular variable bottom topography. K_h is the vertical thermal diffusion coefficient, F_c is the horizontal diffusion term, and C_{source} and C_{sink} represent sources and sinks of C. For the conservative tracer modeling used in this study, no sink/source term is included. In our model, the tracer model is embedded within the hydrodynamic model so that we can conduct "online" tracking, meaning that the tracer model can use instantaneous results of water flow and mixing from every eight-second time step of the hydrodynamic simulation to model the distribution of the effluent plume. This approach provides more accurate results but requires more computational power than "offline" tracking [49], which reads archived hydrodynamic model output (often in an hourly time interval) as input to drive the tracer model.

A conservative tracer is required in simulating plume hydrodynamics so that mass transport and kinetic influences on plume distribution may be separated; conductivity is traditionally applied for this purpose. Here, we utilize nitrate (NO_3-N) as the tracer due to its degree of enrichment proximate to WWTP outfalls relative to ambient lake water (42% and 23% in July and September 2014, respectively, for nitrate and 5% and 2% in July and September 2014, respectively, for conductivity; Figure 4). Additionally, NO_3-N may be considered as approximately conservative over the time interval of measurement used here to characterize plume dimensions. Seasonal surface water nitrate depletion due to phytoplankton nutrient uptake is regularly observed in the Great Lakes [18,50–52]. The rate of nitrate depletion at the study site, determined from contemporary measurements made on four dates in 2014 (5 June, 6 August, 3 September, and 17 September) by the Toronto and Region Conservation Authority, http://arcgis01.trca.on.ca/nswq/,), was 1.2 µg NO_3-N·L^{-1}·day^{-1}. This rate is comparable to that observed in our measurements (1.6 µg NO_3-N·L^{-1}·d^{-1} and is <1% of the range in nitrate levels measured in our single day sampling events. The near-conservative nature of nitrate is also evidenced by the linearity of its relationship with paired measurements of conductivity (Figure 4).

Both field observations and modeled NO_3-N concentrations help us to better define tributary and WWTP plume dimensions. Tributary nitrate concentrations and temperatures were obtained from the Toronto and Region Conservation Authority (TRCA, trca.on.ca). Mean daily flow for the Rouge River and Duffins Creek were obtained from the Environment Canada Water Office (wateroffice.ec.gc.ca), and the flow of Carruthers Creek was estimated by applying a watershed area ratio obtained from the TRCA to the flow data for Duffins Creek. Tributary flows were scaled up from the point of measurement to represent entire watersheds. Time series of mean WWTP effluent flow, temperature, and NO_3-N concentration were obtained from annual wastewater treatment plant reports published by the City of Toronto (web.toronto.ca) and through special requests to the Region of Durham. The Pickering Nuclear Generating Station was included as a point source of effluent (spent cooling water) with data provided by the Region of Durham, ON. The NO_3-N concentration in the two PNGS discharges (PNGS A and PNGS B) was assumed to be equivalent to the mean lake surface (1 m) concentration measured at the two sampling locations nearest to the PNGS outfall.

For the modeling application presented here, NO_3-N baseline concentrations of 355 and 270 $\mu g \cdot L^{-1}$ were applied lakewide (for July and September, respectively). These values were chosen based on concentrations representing the lower fifth percentile of our datasets, i.e., those uninfluenced by tributary and point source discharges. It was recognized that higher constituent concentrations could be present near the western boundaries of the study system, i.e., those potentially impacted by discharges to the west within the GTA. Inspection of field measurements revealed that antecedent meteorological and hydrodynamic conditions (longshore transport) resulted in nitrate levels to the west of our study site well in excess of the baseline condition. This was accommodated by including the NO_3-N discharge of the Ashbridges Bay WWTP (west of the study site; Figure 3 inset) in our model configuration. The plant's flow rate and NO_3-N concentration were obtained from the plant's 2016 Annual Report (published by the City of Toronto; Tables 1 and 2).
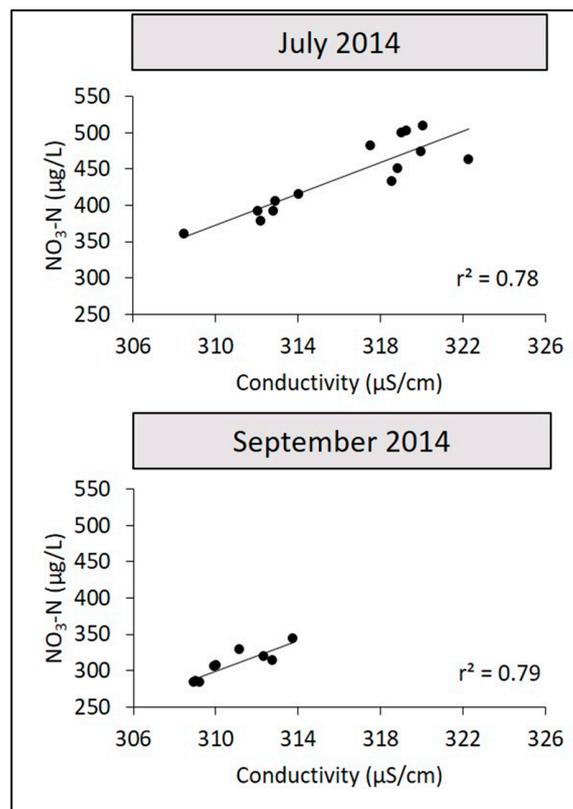

Figure 4. Comparison of transect means (see Figure 2 for transect locations) for NO_3-N and specific conductivity in July and September 2014, respectively. The transect means are calculated as the mean of the vertically averaged concentration at each station within a transect.

2.4. Design of Numerical Experiments

FVCOM is applied in conducting three numerical experiments, corresponding to the steps outlined in *Objectives and Approach*. While the FVCOM/tracer-submodel framework remains constant in all cases, specifics of model application vary and, thus, are described here for each case.

2.4.1. Testing Model Performance by Comparison with Field Measurements

The design for numerical experiments here includes a run (run#1) for the full project period (210 days; 1 March to 30 September 2014) utilizing all tributary and WWTP loads and applied to calibration/confirmation of meteorological data, hydrodynamic results, and tracer concentrations. Simulations were initialized for March 2014 with an initial water temperature of 2 °C (similar to Xue et al. [37]) and run for a spin-up period through June, when summer stratification typically develops [53]. In testing model performance, meteorological conditions and the results of hydrodynamic simulations are

validated with available data from buoy and ADCP measurements, and tracer model results are evaluated against data from two sampling events occurring on 19 July and 9 September 2014 (Section 2). Nitrate loads for tributary and point source inputs were calculated as the product of their individual flow and nitrate concentration (Table 2). As conditions of flow and concentration are relatively stable at wastewater treatment plants, we utilized mean monthly flow and mean monthly concentration. For tributaries, where conditions are more variable, we used mean daily flows. Sampling of tributary concentrations (Toronto Region Conservation Authority) was conducted on only two dates (one in July and one in September); thus, single measurements were utilized there. Model inputs and environmental forcing conditions are summarized in Table 2.

Table 2. Model inputs and environmental forcing conditions used in Finite Volume Community Ocean Model (FVCOM) simulations. Data sources as described in text.

Sources		Daily Flow $(m^3 \cdot s^{-1})$	Outfall Depth (m)	Temp (°C)	NO_3-N $(\mu g \cdot L^{-1})$
Tributaries					
Rouge River	July	0.66–2.37	-	-	444
	Sept	0.95–30.39		-	771
Duffins Creek	July	1.32–1.74	-	-	323
	Sept	1.16–15.05		-	335
Carruthers Creek	July	0.17–0.23	-	-	69
	Sept	0.15–1.99		-	79
Point Sources					
Highland Creek WWTP	July	1.9	11.9	23.1	18,600
	Sept	2.0		22.7	11,900
Duffin Creek WWTP	July	3.7	10	21.1	16,500
	Sept	3.9		18.8	15,800
Corbett Creek WWTP	July	0.5	9	19.5	20,800
	Sept	0.6		21.0	14,900
Ashbridges Bay WWTP	July	7.31	11	20.9	18,500
	Sept	7.31		20.9	18,500
Pickering Nuclear Generation Station					
PNG A	July	49.7	-	22	450
	Sept	49.7		28.2	283
PNG B	July	103.4	-	21	450
	Sept	103.4		28.2	283
Baseline Conditions					
Open Lake	July	-	-	-	355
	Sept	-		-	270

2.4.2. Characterizing Dynamic Plume Behavior

FVCOM is applied here with the linked tracer model to define the plume originating from the three tributary and three point source inputs discharging directly to the study system (Tables 1 and 2, and Figure 2). A generic, conservative tracer is employed so that the impacts of source hydrology (rate of discharge) and receiving water hydrodynamics may be isolated from those associated with biokinetic processes. Initial and boundary conditions assume that no tracer is present in the receiving water. Tracer loads are calculated as the product of the flow for each source and the tracer concentration. In this section, concentration can be normalized equal to one, so that model output is presented as a percentage of the tracer concentration at discharge, an expression that describes the role of physical processes (hydrology and hydrodynamics) in a general fashion subsequently applicable to a broad range of POCs. This mode of expression also facilitates both bounding of the plume and characterization of tracer gradients within the plume. Simulations are performed for stand-alone and multiple sources: the Duffin Creek WWTP to examine variability in the plant's plume position (run#2: 13 days, 9–21 July); Duffins Creek to compare that tributary's footprint during high- and low-flow periods (run#3: high flow, 30 days, 21 March–21 April; run#4: low flow, 30 days, 30 June–30 July) and to examine the nearshore flushing rate (run#5: flushing, 20 days, 10–30 April) and all three WWTPs inputs to quantify plume overlap and the system-wide extent of the combined plumes (run#6: 13 days, 9–21 July).

2.4.3. Evaluating POC Footprint Dimensions in a Regulatory Context

Finally, the model is applied to define the POC footprint of the discharge, i.e., the portion of the plume occupied in meeting the water quality standard, and the degree to which the guidelines for a regulatory mixing zone are met. The analysis is limited to a single discharge, that of the Duffin Creek WWTP, and is applied for three POCs (ammonia nitrogen, total phosphorus, and soluble reactive phosphorus). The resulting footprints are then examined with respect to regulatory guidelines to keep the mixing zone as small as possible and avoid interference with beneficial uses.

3. Results and Discussion

3.1. Testing Model Performance

3.1.1. Simulating Meteorological and Hydrodynamic Conditions

Wind-driven flow plays an important role in governing mass transport in coastal regions. Although the CFSR meteorological forcing used here is considered suitable for lake-wide simulations [37], our first step for this study was to ensure that wind conditions measured at a local buoy were consistent with CFSR output for the coastal region of interest. A comparison of eastward and northward wind components at the study site (Figure 5, upper panel) demonstrates that CFSR-derived data are consistent with buoy-measured winds. Notice that buoy winds were measured at the 5-m level, which was adjusted to wind at the 10-m level based on the formula of log wind profile [54,55],

$$u(z_2) = u(z_1) \times \frac{\ln\left(\frac{z_2-d}{z_0}\right)}{\ln\left(\frac{z_1-d}{z_0}\right)}, \tag{2}$$

where the reference wind speed $u(z_1)$ is measured at height $z_1 = 5$ m, $u(z_2)$ is the wind speed at height $z_2 = 10$ m, z_0 is the roughness length ($z_0 = 0.0002$ m for the water surface), and d is the zero-plane displacement (the height in meters above the ground at which zero wind speed is achieved, assumed to be zero for the water surface).
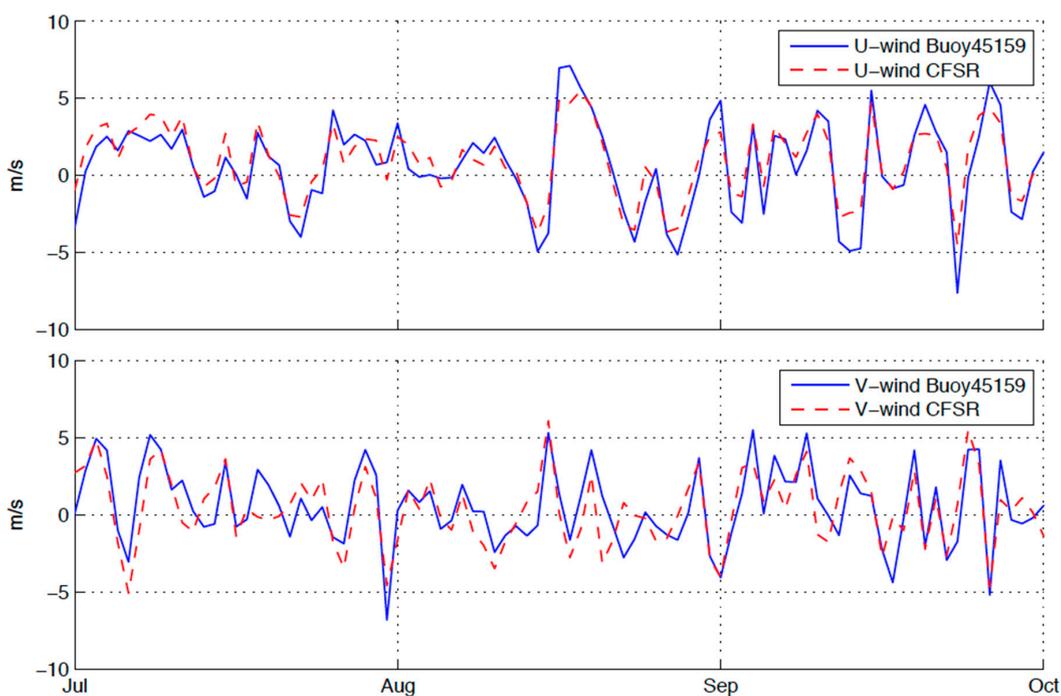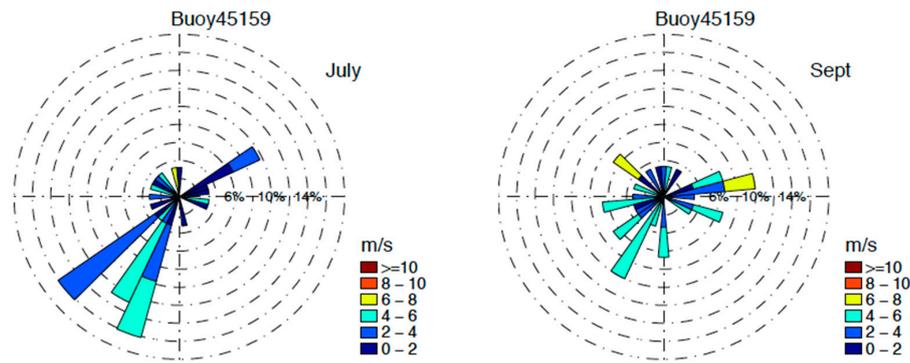

Figure 5. *Cont.*

Figure 5. Upper panel: comparison of the daily averaged wind speeds from NDBC Buoy 45159 and from the Climate Forecast System Reanalysis (CFSR) reanalysis wind speed at the buoy location. Lower panel: wind rose plots based on the same dataset. The length of each "spoke" around the circle represents the frequency (%) with which the wind blows from that direction. Each concentric circle represents a different frequency, increasing from zero at the center to higher frequencies at the outer circles. All wind roses use 16 cardinal directions (e.g., north (N), north-northeast (NNE), northeast (NE), etc.). Wind speeds are presented in 2-m/s bins using the color bar at the lower right.

In July, the prevailing wind (>50% of the time) was from the southwest (a longshore direction) with a daily averaged speed ranging from 2 to 6 $m \cdot s^{-1}$ (Figure 5, lower panel). Northeasterly winds (also longshore) occurred from time to time (10%), while cross-shore winds were observed less frequently. Southwesterly winds remained predominant in September; however, wind direction was generally more random at that time. The wind was generally stronger during September with a typical speed ranging from 4 to 8 $m \cdot s^{-1}$ (Figure 5, lower panel).

Wind and currents in the nearshore of northern Lake Ontario are well correlated. For example, a comparison of the longshore wind component derived from buoy measurements and the alongshore currents measured by the ADCP yielded a correlation coefficient of 0.61, even though the buoy and the ADCP were not at exactly the same locations (the buoy is located farther offshore; Figure 3). In addition, the longshore wind component obtained from the CFSR data and alongshore currents simulated by FVCOM were well correlated ($r = 0.76$); here, both results are taken at the ADCP location. These results suggest that wind patterns significantly affect flow conditions in this region, and that hydrodynamic models will capture realistic flow conditions if quality meteorological forcing is used to drive the model. This conclusion is confirmed by a comparison of flow conditions measured by the ADCP and simulated by FVCOM (Figure 6). Model-simulated current conditions agree well with ADCP measurements for both alongshore and cross-shore flow components (Figure 6). The longshore component varied between $-10 \ cm \cdot s^{-1}$ and $10 \ cm \cdot s^{-1}$ and was much stronger than the cross-shore flow ($<4 \ cm \cdot s^{-1}$) at the near-surface layer (2 m). Synoptic events causing a strong longshore flow were well captured by the model (e.g., 28 July, 12–14 August, 25 August, and 5 September 2014; Figure 6). Longshore flow at the near-surface layer (2 m) shows the largest variability and decreases from surface to bottom due to bottom friction. Cross-shore flows were weak throughout the water column and no significant vertical variability was observed. This result suggests that transport in the longshore direction was much more significant than for the cross-shore.

As thermal conditions also influence flow patterns, we compared model-simulated lake surface temperature (LST) with buoy measurements (Figure 6). Both model results and buoy data show that the LST increased from 9 °C to 20 °C during June. Two cooling events, causing an abrupt and significant drop in temperature in July and August, were captured as well. Throughout September, both observations and model results show that the LST decreases gradually from 20 °C to 15 °C, reflecting typical seasonal cooling. This provides us with confidence in model performance at the local scale of the region of interest, which is critical to the determination of pollutant transport and characterization of plume dynamics. Finally, we note that a similar hydrodynamic model configuration

was applied for lake-wide simulations of the Great Lakes from 2002–2014; model results validated at the basin scale are presented in Xue et al. [10], targeting a coupled lake–atmosphere simulation.
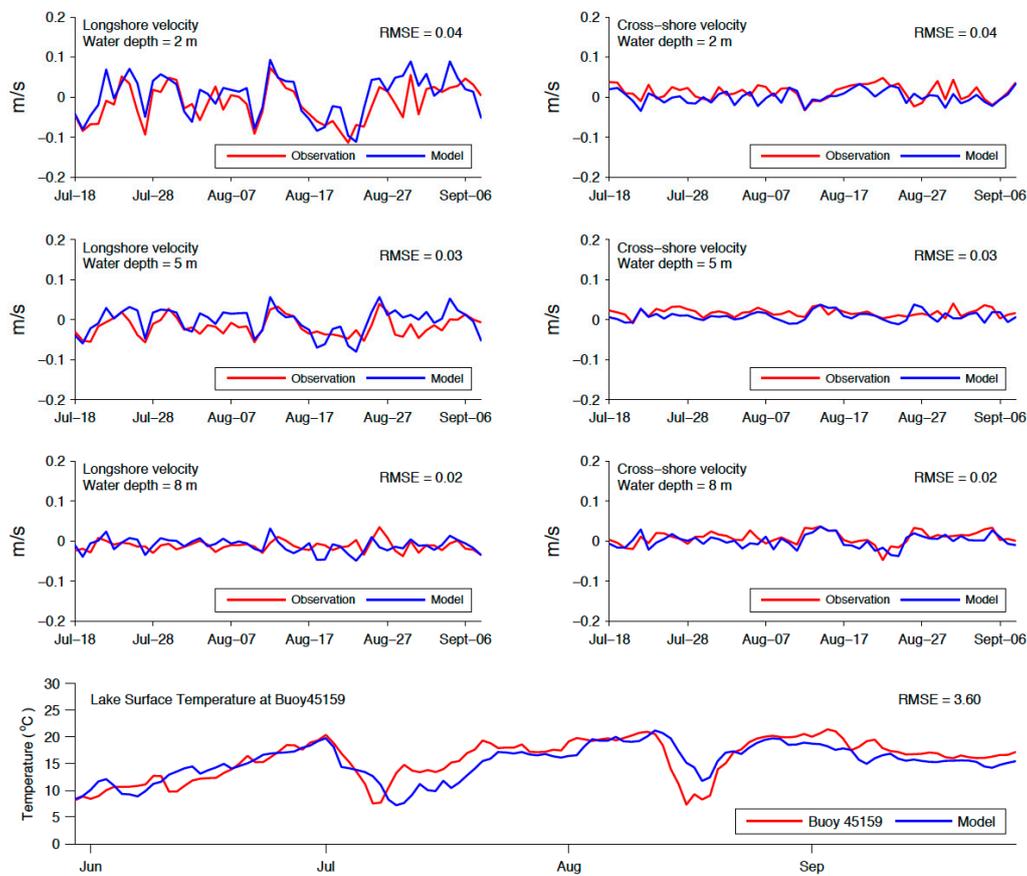

Figure 6. Comparison of model output with ADCP measurements of daily averaged longshore and cross-shore currents at depths of 2 m (near surface), 5 m (middle layer), and 8 m (near bottom). Comparisons of model output and measurements of the daily average lake surface temperature at the NDBC Buoy 45159 location are presented in the bottom panel (only surface water temperature is available at the buoy location).

3.1.2. Simulating Tracer Plume Dimensions

Having demonstrated the efficacy of FVCOM in representing coastal hydrodynamic conditions, attention now turns to the ability of the model to simulate plume dimensions across the study site. Here, we link FVCOM with a soluble tracer model to track the plume associated with tributary and point source discharges. Model performance was first assessed by comparing measured and modeled NO_3-N concentrations (Figure 7) for each sampling transect (see Figure 2). The transect-average concentrations presented here are calculated as the mean of the station-average concentrations making up that transect. Station averages are the means of the vertical profiles measured for each station. The model–data comparison shows that, for the July sampling, the model successfully predicts elevations in NO_3-N levels proximate to the Highland Creek (>450 µg NO_3-N·L^{-1}) and Duffin Creek WWTP (~500 µg NO_3-N·L^{-1}) outfalls and constant, near-baseline levels to the east (~350 µg NO_3-N·L^{-1}) toward the Corbett Creek WWTP outfall. On this occasion, the discharge from the Duffin Creek WWTP is seen to impact a longshore distance of 5 km (reaching 2 km east and 3 km west of the outfall) as evidenced by lower levels of NO_3-N between adjacent areas of WWTP influence (troughs in Figure 7). A similar, yet less clear pattern is seen in results from the September survey, where much less variability in NO_3-N levels is observed across the study site. The model results agree well with observations at sampling locations to the west of the Duffin Creek WWTP outfall except at the westernmost transect,

where the model under-predicts the NO_3-N concentration by ~30 µg·L^{-1} (<10%) in both July and September. To the east of the Duffin Creek WWTP outfall, model results agree well with observations of near-baseline NO_3-N levels with some underestimation at a single transect 4 km east of the Duffin Creek WWTP outfall in September. An objective comparison of modeled and measured transect mean NO_3-N concentrations indicates a good model fit for both the calibration ($r^2 = 0.87$; normalized root-mean-square error (RMSE) = 4%) and confirmation ($r^2 = 0.70$; normalized RMSE = 5%) cases (Figure 7, lower panel).
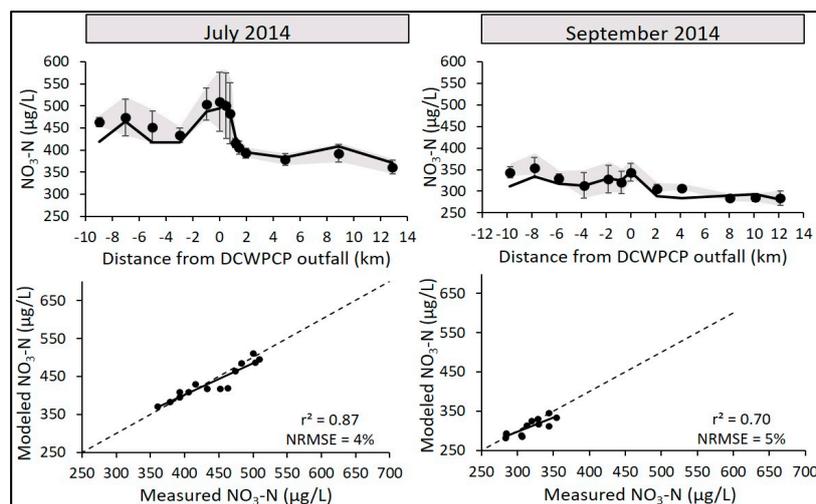
Figure 7. *Top panels*: comparison of transect-mean nitrate concentrations (see Figure 3 for transects) for model results and measurements on 19 July and 9 September 2014. The transect means are calculated as the means of the vertically averaged concentration at each transect station. *Bottom panels*: 1:1 comparison of model results from run#1 to measurements. Solid black lines indicate the best fit between model and data. Dashed lines are a diagonal representing a perfect match. Coefficient of determination (r^2) and normalized root-mean-square error (NRMSE) between model results and measurements were estimated at a significance level of $p = 0.05$. Model results are from run#1.

The transect-average measurements presented above serve well in defining the alongshore extent of point source effluent plumes and the juxtaposition of regions of impact with adjoining regions having constituent concentrations characteristic of the offshore. Further insight regarding plume distributions may be gained through a two-dimensional (2D) spatial representation (Figure 8). It is challenging to capture the details of transient patterns at every station. However, model output and data agree well in defining effluent patterns in both the alongshore and onshore–offshore dimensions. On the dates of simulation, the Duffin Creek and Highland Creek WWTP plumes extend to the west and are gradually attenuated. In the case of the July survey, the model successfully predicts the strong gradient in effluent NO_3-N concentrations near the Duffin Creek WWTP outfall. For a plume represented by NO_3-N concentrations >480 µg·L^{-1}, the effluent is seen to spread ~2 km to the west and in the offshore direction; concentrations immediately to the east of the outfall are much lower, however, resulting in a strong gradient near the point of discharge. The plume may be seen to extend up to ~4 km to the west if defined by a nitrate concentration >435 µg NO_3-N·L^{-1}. The plume extent was slightly less for the Highland Creek WWTP discharge, with a longshore influence of ~1 km based on plume concentrations >480 µg·L^{-1} and 4 km for concentrations >435 µg NO_3-N·L^{-1}. With loads much lower than those of the other study site WWTPs (Table 2), the Corbett Creek WWTP has a much smaller effect on tracer concentrations across the adjoining nearshore. The Corbett Creek WWTP plume is barely evident in the July survey and of modest dimensions in September (Figure 8), following the shoreline to the north and west.

We emphasize that model performance in matching transient data on a point-by-point basis is particularly challenging, as the spatiotemporal variability of effluent constituent concentrations is

extremely high in the vicinity of WWTP discharges. For example, plume concentrations proximate to the Duffin Creek WWTP outfall could vary from more than 500 µg NO_3-N·L^{-1} to levels approaching the lake baseline over a 36-h period (see Figure S1, Supplementary Materials) depending on conditions of advective transport (currents). The agreement of model output and field observations demonstrates the ability of the linked FVCOM-tracer model to predict the extent of plume influence. Specifically, the simulations effectively locate and bound the plumes and characterize the transition regions between discharges, i.e., high concentrations becoming moderate between the Duffin Creek and Highland Creek WWTP outfalls and moderate concentrations becoming low between the Duffin Creek and Corbett Creek WWTP discharges.
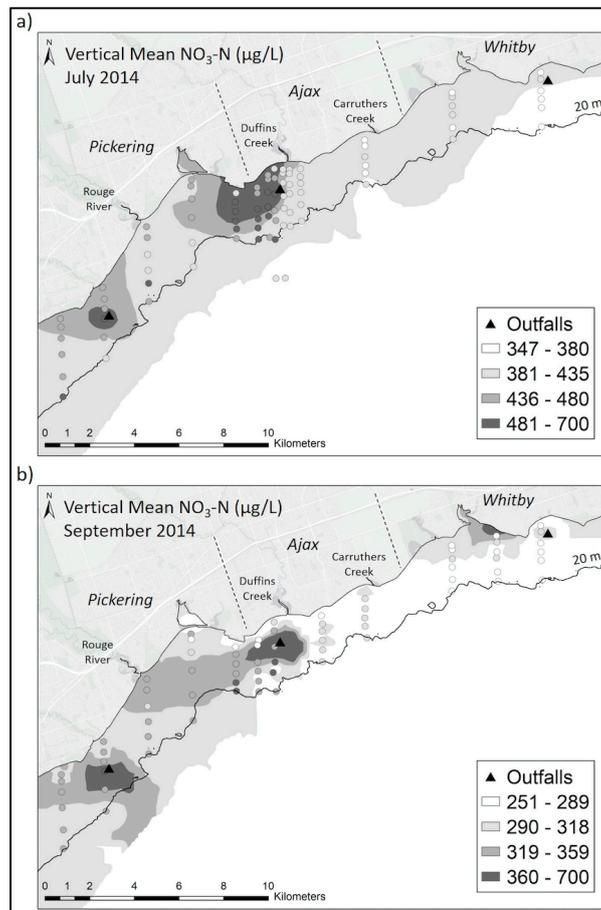
Figure 8. Spatial comparison of vertically averaged measured (circles) and modeled (filled contours) NO_3-N concentration on (**a**) 19 July 2014 and on (**b**) 9 September 2014. Note: The modeled contours were produced using empirical Bayesian kriging (July) and ordinary kriging (September) interpolation methods in ArcMap and using vertically averaged model output at the sampling stations. To avoid extrapolation, contours were trimmed along the 36-m depth contour. Model results are from run#1.

3.2. Characterizing Dynamic Plume Behavior

Characterization of tributary and point source plumes is complicated by the fact these discharges to the nearshore are continuously present and highly dynamic with respect to position: horizontally as driven by constantly shifting coastal currents and vertically as discharges seek a position of density equilibrium in a seasonally warming and cooling water column. Monitoring and modeling results presented to this point (Figures 7 and 8) represent a plume as only a snapshot in time. Over a time frame of days, tributary and point source plumes distribute their constituents across the nearshore in a manner that may be likened to a stationary source (gas stack) discharging to an atmosphere with variable wind speed and direction. The dynamic nature of plumes may be illustrated by performing

simulations over a period longer than the snapshot (here, three simulation results within seven days are selected to illustrate strong variability in plume position), thus incorporating variability in current speed and direction. An FVCOM simulation of this phenomenon is performed using the Duffin Creek WWTP outflow for July 2014 (Table 2).

Simulation results illustrate the dynamic behavior of the Duffin Creek WWTP discharge upon entry to the lake (Figure 9), with plume location reversing direction in response to changes in current structure. Over the period of simulation, the WWTP plume tracks east → west on 12 July, is centrally located on 15 July, and tracks west → east on 19 July; Figure 9). This dynamic behavior applies to both tributary and point source discharges and persists throughout the year. Thus, from an ecosystem management perspective, quantification of plume dimensions (mixing zones in a regulatory context) must accommodate this variability, with the resulting plume describing the entire region influenced by the discharge.
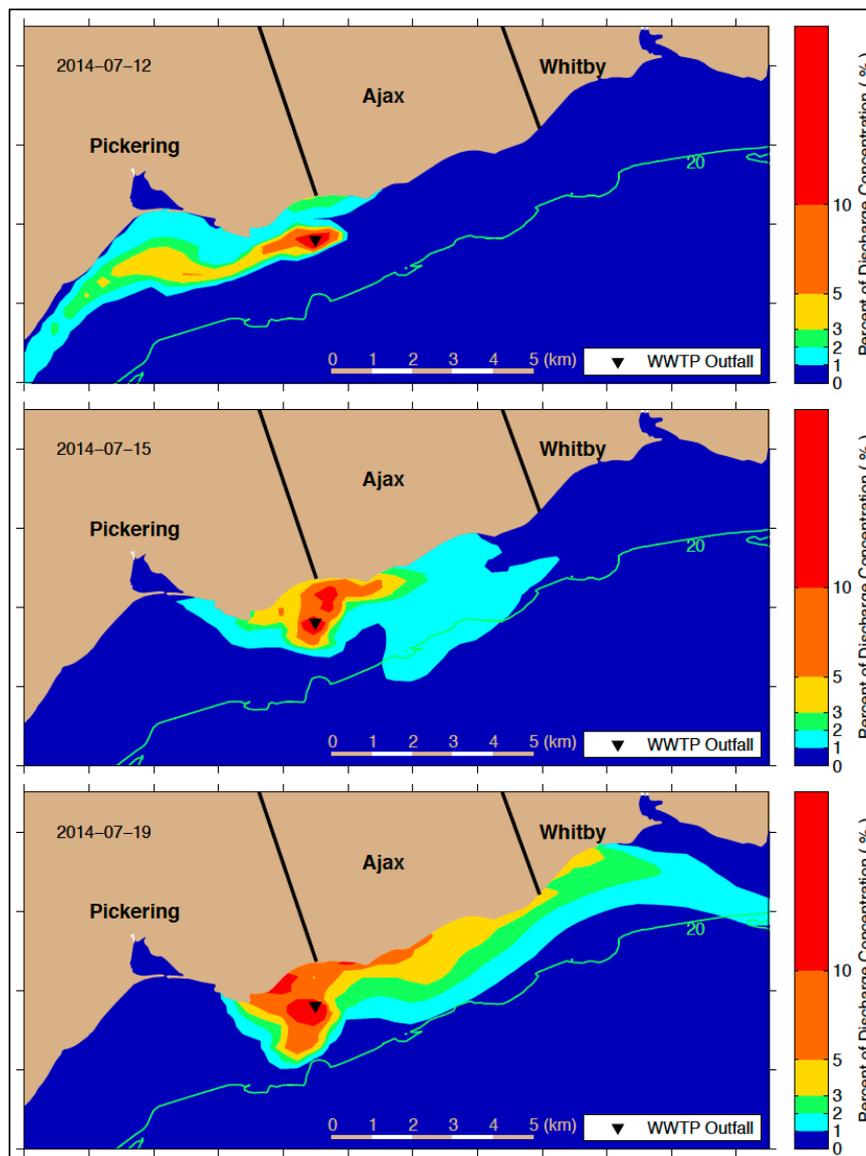

Figure 9. Simulated conservative tracer concentration, averaged over the water column and over the day and expressed as a percentage of the discharge concentration. Results illustrate variation in the Duffin Creek WWTP plume for three dates in 2014. The green line is the 20-m depth representing the approximate lakeward extent of colonization by *Cladophora* and taken as the separation of nearshore and offshore waters. Model results are from run#2.

3.2.1. Tributary Inputs

The annual total phosphorus loads for the three tributaries discharging to the study site, the Rouge River, Duffins Creek, and Carruthers Creek, rank 10th, 16th, and 51st, respectively, among the 95 Canadian tributaries to Lake Ontario tabulated for 2008 by Makarewicz et al. [19]. Annual total phosphorus loads for Duffins Creek were estimated to range from approximately 10 to 90 metric tons per year [26], with the upper bound approaching the annual load for the Duffin Creek WWTP (mean of 138 metric tons per year, 2012–2016 [56]). This may be interpreted as meaning that Duffins Creek and the Duffin Creek WWTP are of comparable importance in mediating local nearshore nutrient concentrations. However, tributary loads exhibit significant intra-annual variability, reflecting seasonality in constituent concentration and, particularly, flow (Figure 10a).
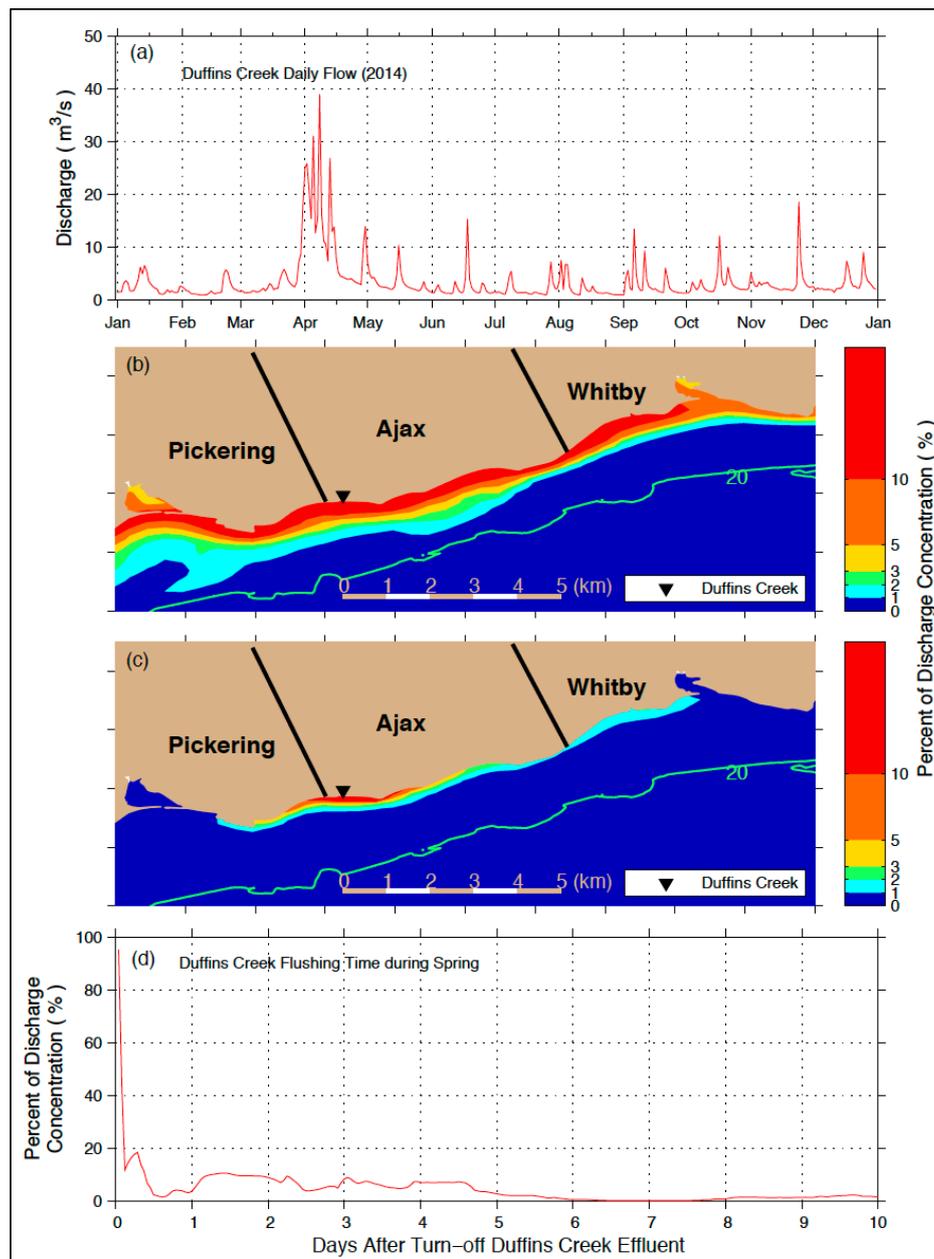

Figure 10. Model inputs and results for tributary simulations: (**a**) Duffin Creek flows for 2014, (**b**) Duffin Creek plume for high-flow conditions, 4–10 April 2014 (model results are from run#3), (**c**) Duffin Creek plume for low-flow conditions, 13–19 July 2014 (model results are from run#4), and (**d**) purging of the Duffins Creek plume from nearshore waters (model results are from run#5).

Two FVCOM simulations (run#3 and#4) are performed here for Duffins Creek representing early spring (high flow) and late spring and summer (low flow) conditions. It is evident from these simulations that the seasonal decline in tributary flow (Figure 10a) and attendant reduction in load (Table 2) result in plume areas (calculated for concentrations C ≥ 1% of the discharge level) that differ by an order of magnitude for the two periods: ~4800 ha for early spring, high-flow (March–April) conditions (Figure 10b) and ~370 ha for late spring–summer, low-flow (May–July) conditions (Figure 10c). Model runs were then continued for 20 days, reducing the tributary load to zero, to quantify the purging time of constituent concentrations from the nearshore over the high-flow → low-flow transition (run#5). The simulation demonstrates that nearshore constituent concentrations characteristic of the high-flow period (Figure 10a) are purged (<1% remaining) from the system in 6–7 days (Figure 10d) and are, thus, not a critical driver of the nutrient–alga (e.g., phosphorus–*Cladophora*) dynamic during the May–June growth season. This analysis may be extended to tributary wet-weather discharges during the growing season, where purging would limit the residence of their impact to several days. We conclude that the influence of tributaries on nutrient conditions during the interval of *Cladophora* growth is limited to the extreme nearshore at the point where the tributary enters the lake. It is noted, however, that discharges from larger tributaries to Lake Ontario (e.g., the Genesee River at Rochester, New York (NY)) likely maintain a significant plume (and are, thus, a driving force) even in the summer.

3.2.2. Point Source Inputs

The annual total phosphorus loads for the WWTP effluents received by the study site (Highland Creek, Duffin Creek and Corbett Creek) rank second, seventh, and ninth among the 38 Canadian plants discharging to Lake Ontario, as tabulated for 2008 by Makarewicz et al. [19]. Unlike tributaries, effluent discharges from WWTPs exhibit relatively constant flows over the year; however, like all discharges to the nearshore, plume position varies dynamically under the influence of coastal jets (Figure 9). WWTP plume dimensions and the interaction of juxtaposed effluent discharges were explored by performing a 13-day FVCOM run (run#6) using the meteorological and mass transport conditions of 9–21 July 2014. WWTP effluent loads were calculated as the product of flow (Table 2) and the conservative tracer concentration (assumed equal to one and identical for each input). Model output is presented as a percentage of the tracer concentration at discharge, thus representing the interplay of discharge rate and ambient mass transport in determining plume distribution (Figure 11).
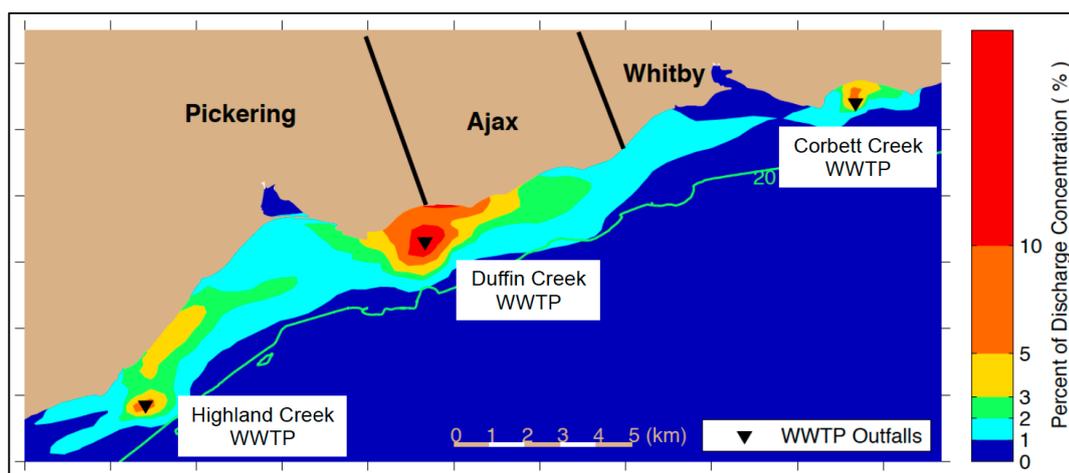

Figure 11. Conservative tracer concentration for a seven-day interval (13–19 July 2014), averaged over the water column and over the simulation period and expressed as a percentage of the discharge concentration. Results illustrate the domain of the plumes and their confluence to the west and separation to the east. The green line is the 20-m depth representing the approximate lakeward extent of colonization by *Cladophora* and taken as the separation of nearshore and offshore waters. Model results are from run#6.

As anticipated, the dimensions of the WWTP plumes are proportional to their loads: Duffin Creek > Highland Creek > Corbett Creek (Figure 11). The Duffin Creek WWTP plume, defined by C ≥ 2%, extends ~5 km to the east and ~3 km to the west of the outfall. The C ≥ 2% plume for the Highland Creek WWTP discharge extends ~4 km to the east and ~1 km to the west, a reduction in plume dimensions, compared with the Duffin Creek WWTP, consistent with the difference in plant flows. Similarly, the C ≥ 2% plume for the considerably smaller Corbett Creek WWTP extends ~1 km to both the east and west. The C ≥ 2% plume for the Duffin Creek and Highland Creek WWTPs extends across a significant portion of the *Cladophora* growth habitat (20 m; lakeward boundary defined by the green line in Figure 11). A value of C ≥ 1% is taken here to represent the outer boundary of the plume, i.e., the confluence of the plume with the offshore boundary concentration (here, 0%). Plume dimensions are much larger for the C ≥ 1% plume boundary as ambient turbulence works to further dilute the point source discharges. The margin of the Duffin Creek WWTP plume defined by C ≥ 1% extends ~10 km to the east and likely a similar distance to the west, although this westward extent is difficult to isolate in a multi-source model run due to the juxtaposition of the Duffin Creek and Highland Creek WWTP plumes (Figure 11). The C ≥ 1% plume for the Highland Creek discharge extends ~3 km to the west, while its eastward extent is not discernable, again due to confluence with the Duffin Creek WWTP plume. The Corbett Creek WWTP plume extends 2 km to the west and ~2 km to the east, a smaller extent, again due to its smaller discharge. Perhaps most striking is the result demonstrating that the C ≥ 1% boundary for the two largest WWTPs extends lakeward, fully across the nearshore zone to the offshore edge of *Cladophora* growth habitat. This, considered in the context of the "unbroken urban landscape" of Rao et al. [17], begins to bring the implications of point source management for control of nuisance growth of *Cladophora* into clearer focus.

3.2.3. Evaluating POC Footprint Dimensions in a Regulatory Context

The offshore discharge of WWTP effluents in the Great Lakes is regulated through the concept of a mixing zone. In this portion of the nearshore environment, segregated from the general region protected for unlimited use, water quality criteria may be exceeded [12,16]. The adoption of a mixing zone concept recognizes the limitations of mandating that wastes be treated to the level of water quality standards, but also that enlargement of the mixing zone not be used as an alternative to reasonable and practical treatment [16].

Evaluation of a discharge to the nearshore with respect to regulatory mixing zone guidelines requires that the dimensions of the effluent plume and POC-specific footprint(s) be established. Here, we describe a generic means for characterizing plume and footprint dimensions, yielding a first approximation of compliance with regulatory guidelines. As previously defined, the POC footprint is the portion of the plume in which the water column concentration exceeds the water quality standard. The footprint boundary may be determined through calculation of D, the dilution (as a percentage of the effluent concentration) required to meet a POC-specific water quality standard through ambient mixing,

$$D = \frac{C_{effluent} - C_{standard}}{C_{effluent}} \times 100, \tag{3}$$

where $C_{effluent}$ is the POC concentration at the point of discharge, and $C_{standard}$ is the POC-specific water quality standard. Note that the determination of D does not involve the FVCOM-tracer model, but rather performs the calculation directly based on two user-specified variables ($C_{effluent}$ and $C_{standard}$).

Values of $C_{effluent}$ and $C_{standard}$ are specified and values of D calculated (Table 3) for three POCs common to wastewater treatment facilities such as the Duffin Creek WWTP. Two of these, total ammonia nitrogen (TAN) and total phosphorus (TP), are traditional pollutants presently regulated in a mixing zone context for point source discharges to Great Lakes waters [12,16]. The third, soluble reactive phosphorus, is a presently unattended POC mandated for management of nuisance algal growth under the Great Lakes Water Quality Agreement. Values of $C_{standard}$ for TAN (500 μg N/L) and TP (20 μg P/L) are those specified by the Ministry of the Environment (MOE) [16] (*Provincial Water*

Quality Objectives). No regulatory standard is currently established for SRP. A value of $C_{standard}$ for SRP (1.5 µg P/L) was calculated using the Great Lakes *Cladophora* Model v2 [57] and represents the upper boundary for P-limited growth of *Cladophora*. This SRP concentration is consistent with estimates offered previously by Canale and Auer [58] (<2 µg SRP/L), Tomlinson et al. [57] (<1 µg SRP/L), and the Targets Task Team [59] (0.9 µg SRP/L). Values for $C_{effluent}$ for TAN are those published in the WWTP's *Annual Performance Report* for 2014 [60] and those for TP and SRP are the means of average annual concentrations for 2012–2016 published in the WWTP's *Phosphorus Reduction Action Plan* [56].

Table 3. Values of $C_{effluent}$, $C_{standard}$ and corresponding D (see Section 3.2.3 for details) for three POCs common to wastewater treatment facilities such as the Duffin Creek WWTP.

Constituent	$C_{standard}$ (mg·L^{-1})	$C_{effluent}$ (mg·L^{-1})	D (%)
Total Ammonia Nitrogen, as N	500	1800	72.2
Total Phosphorus, as P	20	422	95.3
Soluble Reactive Phosphorus, as P	1.5	232	99.4

Recalling that the footprint is defined as the region where the POC concentration exceeds the water quality standard, it follows that the value of D circumscribes the footprint boundary within the plume dilution field (see Figure 1). It, thus, remains to establish the spatial scale over which the required dilution occurs, i.e., what is the size of the POC footprint? The role of the FVCOM-tracer model is to provide a map of the plume dilution field (see Figure 1), where 0% dilution occurs at the point of effluent discharge. The value of D is then mapped onto the FVCOM-tracer model plume dilution field to define the three POC footprints (Figure 12). For a value of D $\rightarrow$ 0, little (or no) dilution is required to constrain the footprint to dimensions consistent with regulatory mixing zone guidelines. As the difference between $C_{standard}$ and $C_{effluent}$ increases, D becomes larger, more dilution is required, and the POC-specific footprint comes to occupy a larger portion of the plume (Table 3 and Figure 12).
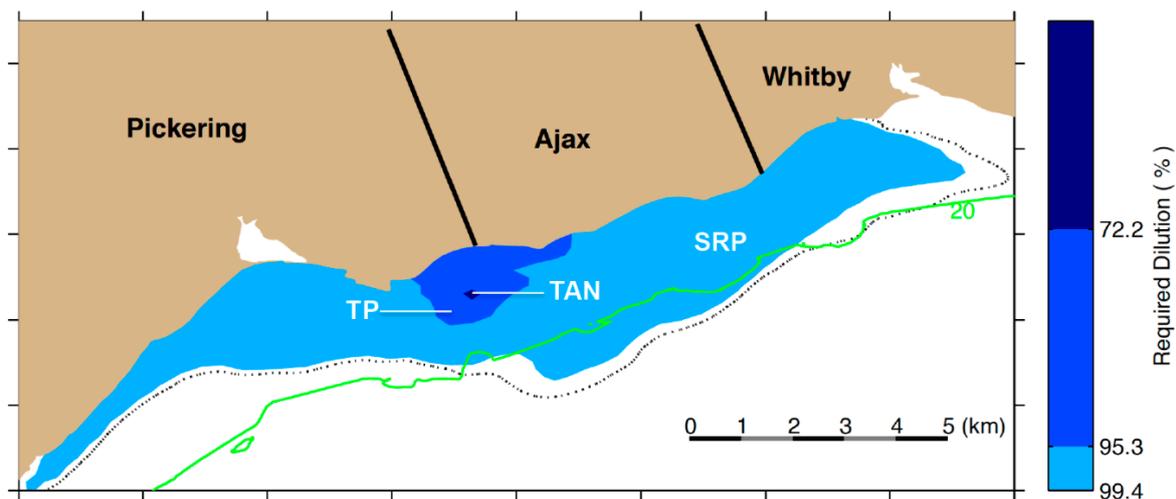

Figure 12. Model-predicted conservative tracer footprints for three pollutants of concern discharged by the Duffin Creek WWTP. Results are water column averages for a seven-day (13–19 July 2014) continuous discharge. The dashed black line identifies the extent of the effluent plume, defined here as a 99.5% reduction from the effluent concentration. Footprint boundaries, corresponding to pollutant of concern (POC)-specific D values (Table 3), circumscribe the area where in-lake POC concentrations exceed the water quality standard. The green line is the 20-m depth representing the lakeward extent of colonization by *Cladophora* [24] and approximating the accepted separation of nearshore and offshore waters [5,6,22]. Model results are from run#2.

The smallest footprint is that for TAN (<0.2 km × 0.2 km; ~4 ha). While requirements relating to mixing zones are developed on a case-by-case basis [16], these dimensions are likely consistent with the regulatory mixing zone guidance to minimize interference with lost beneficial uses. The next largest footprint is that for TP (<2 km × 2 km; ~342 ha), which has an area more than 85 times that for TAN. With dimensions of ~17 km × 2.5 km and an area of ~3708 ha, the SRP footprint is even larger (more than 900 times that for TAN) and extends significantly into the far-field (Figure 12). Thus, the footprint area for SRP approaches one (TP) to two (TAN) orders of magnitude greater than mixing zones presently considered to be acceptable in a regulatory context (TP and TAN [23]). Over much of its extent, particularly in the Ajax nearshore, the footprint fully engages and essentially overlays habitat colonized by *Cladophora* (Figure 12).

4. Conclusions: Management Insights

In this study, we developed a linked hydrodynamic tracer model for Lake Ontario with a high degree of resolution for the region of interest in the northern coastal zone of the lake. Model results show a reasonable agreement with observed hydrodynamic conditions and satisfactorily simulate plume dimensions observed during sampling events. Using this validated model, we developed a generic approach for providing estimates of selected POC footprint dimensions defined by the ratio of water quality standards to effluent discharge concentrations. The generic approach has the advantage of being broadly applicable to a variety of POCs, but is a first-approximation tool offering less accuracy than a POC-specific biokinetic model. We consider these to be estimates to a first approximation as we utilize a conservative tracer to identify the POC footprint for a given source hydrology (WWTP rate of discharge) and receiving water hydrodynamic conditions, isolated from attendant biokinetic processes. If the dimensions of the footprint do not conform to the regulatory guidance for an initial mixing zone, it indicates additional efforts (e.g., extension of the discharge further offshore or reduction of effluent POC concentrations) may be needed to reduce the footprint.

These results, treating POCs as conservative substances to target mass transport processes, indicate that the previously unattended SRP POC will not meet the guidelines for mixing zone-based regulation with current treatment technologies. Since there is a much greater difference between $C_{standard}$ and $C_{effluent}$ for SRP than for TAN or TP (Equation (3), Table 3), the footprint for SRP is much larger than that for TAN and TP (Figure 12) and a greater reduction in $C_{effluent}$ (D = 99.4%) is necessary. These findings confirm, as a first approximation, our hypothesis that a shift in management focus to the Lake Ontario nearshore will reveal a necessity to reassess the impact of POC plumes with respect to regulatory guidelines for coastal waters. To achieve compliance with more stringent standards in nearshore applications, the footprints for previously unattended and emerging POCs may require advanced treatment to maintain compliance in a regulatory context.

The variation in footprints dimensions presented here for TAN, TP, and SRP demonstrate that management challenges may lie ahead in meeting the "as small as possible" and avoidance of "interference with beneficial uses" features of a mixing zone strategy for the nearshore [12,16]. For example, while the TAN and TP management objectives are likely achieved, that for SRP remains challenging in the context of controlling nuisance algal growth. The transition in focus from the open lake to the nearshore will require separation of effluent plumes from areas colonized by *Cladophora*, an alga stimulated by elevated levels of soluble reactive phosphorus and presently growing at nuisance levels in the study area. Simulations performed here demonstrate that the present engineering design of the Duffin Creek WWTP may not be capable of accomplishing that separation.

The present WWTP discharge is located ~1 km offshore and has a footprint with a lakeward boundary reaching 2–3 km offshore (Figure 12). Across much of its longshore dimension, the footprint fully engages and even overlays colonizable *Cladophora* habitat (Figure 12). The outfall extension option would require that the discharge be sited such that its footprint becomes separated from *Cladophora* habitat (i.e., at depths greater than ~25 m, uncolonizable by the alga due to near-bottom light availability [24]), with a margin of safety. The required offshore distance could be established using the

modeling platform applied here for determining plume and footprint dimensions. Technologies capable of supporting the second option, enhanced treatment, are presently available. Tertiary treatment at the Metropolitan Syracuse (NY) Wastewater Treatment Plant, discharging to Lake Ontario via the Seneca and Oswego Rivers, maintained those exceptional levels of SRP removal for more than a decade [61].

The results presented here represent the critical first step in engineering design of a physical (hydrologic, hydrodynamic) foundation for modeling effluent plume and POC footprint dimensions. The second step in design is to apply a coupled hydrodynamic-biokinetic model to accommodate the non-conservative nature of a target POC (e.g., soluble reactive phosphorus with FVCOM-GEM [62,63]). The role of biokinetics is well recognized in mediating plume attenuation in traditional POCs (e.g., nitrification of ammonia nitrogen, cell mortality in *Escherichia coli*, and settling for total phosphorus). That role is less clear for the soluble reactive phosphorus POC where the interplay of biokinetic source (e.g., SRP excretion by invasive dreissenid mussels) and sink terms (e.g., SRP uptake by phytoplankton) may be appropriately considered. Field monitoring and mathematical modeling studies conducted along the Pickering → Ajax → Whitby nearshore revealed no apparent coupling of local phytoplankton growth with individual point source discharges of phosphorus [11,27] and found *Cladophora* biomass density to be weakly correlated with dreissenid abundance [27]. Additionally, Leon et al. [11] reported that their model was able to predict major water quality variables related to nuisance algae growth without inclusion of dreissenid mussels and associated phosphorus cycling. Nonetheless, the significance of biokinetic processes is of sufficient potential in relation to plume/footprint dimensions and, thus, management approaches to merit further attention. We conclude that our results represent a first step, pointing to the potential need for a step change in management practices addressing lost beneficial use as the technologies of the 1970s reach their practical design limits along this "almost unbroken urban landscape" of the Lake Ontario nearshore [17].

References

1. Williamson, J.A. *The Inland Seas of North America; and the Natural and Industrial Productions of Canada with the Real Foundations for Its Future Prosperity*; H. Ramsay: Kingston, ON, Canada, 1854.
2. Csanady, G.T. Hydrodynamics of Large Lakes. *Ann. Rev. Fluid Mech.* **1975**, *7*, 357–386. [CrossRef]
3. Csanady, G.T. Milestones of Research on the Physical Limnology of the Great-Lakes. *J. Great Lakes Res.* **1984**, *10*, 114–125. [CrossRef]
4. Rao, Y.R.; Schwab, D.J. Transport and mixing between the coastal and offshore waters in the great lakes: A review. *J. Great Lakes Res.* **2007**, *33*, 202–218. [CrossRef]
5. Csanady, G.T. The Coastal Boundary Layer in Lake Ontario. Part I: The Spring Regime. *J. Phy. Oceanogr.* **1972**, *2*, 41–53. [CrossRef]

6. Csanady, G.T. The Coastal Boundary Layer in Lake Ontario: Part II. The Summer-Fall Regime. *J. Phy. Oceanogr.* **1972**, *2*, 168–176. [CrossRef]

7. Plew, D.R.; Zeldis, J.R.; Shankar, U.; Elliott, A.H. Using Simple Dilution Models to Predict New Zealand Estuarine Water Quality. *Estuar. Coast.* **2018**, *41*, 1643–1659. [CrossRef]

8. Beletsky, D.; Schwab, D.J. Modeling circulation and thermal structure in Lake Michigan: Annual cycle and interannual variability. *J. Geophys. Res. Ocean.* **2001**, *106*, 19745–19771. [CrossRef]

9. Xue, P.F.; Schwab, D.J.; Sawtell, R.W.; Sayers, M.J.; Shuchman, R.A.; Fahnenstiel, G.L. A particle-tracking technique for spatial and temporal interpolation of satellite images applied to Lake Superior chlorophyll measurements. *J. Great Lakes Res.* **2017**, *43*, 1–13. [CrossRef]

10. Xue, P.F.; Pal, J.S.; Ye, X.Y.; Lenters, J.D.; Huang, C.F.; Chu, P.Y. Improving the Simulation of Large Lakes in Regional Climate Modeling: Two-Way Lake-Atmosphere Coupling with a 3D Hydrodynamic Model of the Great Lakes. *J. Clim.* **2017**, *30*, 1605–1627. [CrossRef]

11. Leon, L.F.; Smith, R.E.H.; Malkin, S.Y.; Depew, D.; Hipsey, M.R.; Antenucci, J.P.; Higgins, S.N.; Hecky, R.E.; Rao, R.Y. Nested 3D modeling of the spatial dynamics of nutrients and phytoplankton in a Lake Ontario nearshore zone. *J. Great Lakes Res.* **2012**, *38*, 171–183. [CrossRef]

12. U.S. Environmental Protection Agency (U.S.EPA). *Dilution Models for Effluent Discharges*, 3rd ed.; EPA/600/R-94/086; Office of Research and Development: Washington, DC, USA, 1994.

13. Anderson, E.J.; Fujisaki-Manome, A.; Kessler, J.; Lang, G.A.; Chu, P.Y.; Kelley, J.G.; Chen, Y.; Wang, J. Ice Forecasting in the Next-Generation Great Lakes Operational Forecast System (GLOFS). *J. Mar. Sci. Eng.* **2018**, *6*, 123. [CrossRef]

14. Xue, P.; Schwab, D.J.; Zhou, X.; Huang, C.; Kibler, R.; Ye, X. A Hybrid Lagrangian–Eulerian Particle Model for Ecosystem Simulation. *J. Mar. Sci. Eng.* **2018**, *6*, 109. [CrossRef]

15. Roberts, P.J.W. Engineering of Ocean Outfalls. In *The Role of the Oceans as a Waste Disposal Option*; Kullenberg, G., Ed.; Springer: Dordrecht, The Netherlands, 1986; pp. 73–109.

16. Ministry of the Environment (MOE). *Water Management Policies, Guidelines and Provincial Water Quality Objectives of the Ministry of Environment and Energy*; Queen's Printer for Ontario: Toronto, ON, Canada, 1994.

17. Rao, Y.R.; Murthy, R.C.; Chiocchio, F.; Skafel, M.G.; Charlton, M.N. Impact of proposed Burlington and Hamilton sewage discharges in western Lake Ontario. *Water Qual. Res. J. Can.* **2003**, *38*, 627–645. [CrossRef]

18. Neilson, M.A.; Stevens, R.J.J. Spatial Heterogeneity of Nutrients and Organic-Matter in Lake-Ontario. *Can. J. Fish. Aqua. Sci.* **1987**, *44*, 2192–2203. [CrossRef]

19. Makarewicz, J.C.; Booty, W.G.; Bowen, G.S. Tributary phosphorus loading to Lake Ontario. *J. Great Lakes Res.* **2012**, *38*, 14–20. [CrossRef]

20. Higgins, S.N.; Pennuto, C.M.; Howell, E.T.; Lewis, T.W.; Makarewicz, J.C. Urban influences on Cladophora blooms in Lake Ontario. *J. Great Lakes Res.* **2012**, *38*, 116–123. [CrossRef]

21. Howell, E.T. Cladophora (green algae) and dreissenid mussels over a nutrient loading gradient on the north shore of Lake Ontario. *J. Great Lakes Res.* **2018**, *44*, 86–104. [CrossRef]

22. Yurista, P.M.; Kelly, J.R.; Miller, S.; Van Alstine, J. Lake Ontario: Nearshore conditions and variability in water quality parameters. *J. Great Lakes Res.* **2012**, *38*, 133–145. [CrossRef]

23. CH2M HILL. *Class Environmental Assessment to Address Outfall Capacity Limitations at the Duffin Creek Water Pollution Control Plant. Environmental Study Report. Prepared for The Regional Municipalities of York and Durham by CH2M HILL*; CH2M HILL Canada Limited: Toronto, ON, Canada, 2013.

24. Kuczynski, A.; Auer, M.T.; Brooks, C.N.; Grimm, A.G. The Cladophora resurgence in Lake Ontario: characterization and implications for management. *Can. J. Fish. Aqua. Sci.* **2016**, *73*, 999–1013. [CrossRef]

25. Auer, M.T.; Tomlinson, L.M.; Higgins, S.N.; Malkin, S.Y.; Howell, E.T.; Bootsma, H.A. Great Lakes Cladophora in the 21st century: same algae-different ecosystem. *J. Great Lakes Res.* **2010**, *36*, 248–255. [CrossRef]

26. Booty, W.G.; Wong, I.; Bowen, G.S.; Fong, P.; McCrimmon, C.; Leon, L. Loading estimate methods to support integrated watershed-lake modelling: Duffins Creek, Lake Ontario. *Water Qual. Res. J. Can.* **2014**, *49*, 179–191. [CrossRef]

27. Howell, E.T. Influences on Water Quality and Abundance of Cladophora, a Shore-Fouling Green Algae, over Urban Shoreline in Lake Ontario. *Water* **2018**, *10*, 1569. [CrossRef]

28. Howell, E.T.; Chomicki, K.M.; Kaltenecker, G. Tributary discharge, lake circulation and lake biology as drivers of water quality in the Canadian Nearshore of Lake Ontario. *J. Great Lakes Res.* **2012**, *38*, 47–61. [CrossRef]

29. Howell, E.T.; Chomicki, K.M.; Kaltenecker, G. Patterns in water quality on Canadian shores of Lake Ontario: Correspondence with proximity to land and level of urbanization. *J. Great Lakes Res.* **2012**, *38*, 32–46. [CrossRef]

30. Leon, L.F.; Smith, R.E.; Malkin, S.; Depew, D.; Hecky, R.E. *Modeling and Analysis of Cladophora Dynamics and Their Relationship to Local Nutrient Sources in A Nearshore Segment of Lake Ontario, #4253501. Final Report for OPG*; University of Waterloo: Waterloo, ON, Canada, 2009; p. 64.

31. Martin, G.M. Nutrient sources for excessive growth of benthic algae in Lake Ontario as inferred by the distribution of SRP. M.S. Thesis, UWSpace, University of Waterloo, Waterloo, ON, Canada, 2010.

32. Chen, C.S.; Liu, H.D.; Beardsley, R.C. An unstructured grid, finite-volume, three-dimensional, primitive equations ocean model: Application to coastal ocean and estuaries. *J. Atmosph. Ocean. Technol.* **2003**, *20*, 159–186. [CrossRef]

33. Chen, C.S.; Beardsley, R.C.; Cowles, G. An unstructured grid, finite-volume coastal ocean model (FVCOM) system. *Oceanography* **2006**, *19*, 78–89. [CrossRef]

34. Xue, P.F.; Chen, C.S.; Beardsley, R.C. Observing system simulation experiments of dissolved oxygen monitoring in Massachusetts Bay. *J. Geophys. Res. Ocean.* **2012**, *117*. [CrossRef]

35. Anderson, E.J.; Bechle, A.J.; Wu, C.H.; Schwab, D.J.; Mann, G.E.; Lombardy, K.A. Reconstruction of a meteotsunami in Lake Erie on 27 May 2012: Roles of atmospheric conditions on hydrodynamic response in enclosed basins. *J. Geophys. Res. Ocean.* **2015**, *120*, 8020–8038. [CrossRef]

36. Safaie, A.; Wendzel, A.; Ge, Z.F.; Nevers, M.B.; Whitman, R.L.; Corsi, S.R.; Phanikumar, M.S. Comparative Evaluation of Statistical and Mechanistic Models of Escherichia coli at Beaches in Southern Lake Michigan. *Environ. Sci. Technol.* **2016**, *50*, 2442–2449. [CrossRef]

37. Xue, P.F.; Schwab, D.J.; Hu, S. An investigation of the thermal response to meteorological forcing in a hydrodynamic model of Lake Superior. *J. Geophys. Res. Ocean.* **2015**, *120*, 5233–5253. [CrossRef]

38. Ye, X.Y.; Anderson, E.J.; Chu, P.Y.; Huang, C.F.; Xue, P.F. Impact of Water Mixing and Ice Formation on the Warming of Lake Superior: A Model-guided Mechanism Study. *Limnol. Oceanogr.* **2019**, *64*, 558–574. [CrossRef]

39. Xue, P.F.; Chen, C.S.; Qi, J.H.; Beardsley, R.C.; Tian, R.C.; Zhao, L.Z.; Lin, H.C. Mechanism studies of seasonal variability of dissolved oxygen in Mass Bay: A multi-scale FVCOM/UG-RCA application. *J. Mar. Sys.* **2014**, *131*, 102–119. [CrossRef]

40. Xue, P.F.; Eltahir, E.A.B. Estimation of the Heat and Water Budgets of the Persian (Arabian) Gulf Using a Regional Climate Model. *J. Clim.* **2015**, *28*, 5041–5062. [CrossRef]

41. Schwab, D.J.; Bedford, K.W. Initial Implementation of the Great Lakes Forecasting System: A Real-Time System for Predicting Lake Circulation and Thermal Structure. *Water Qual. Res. J.* **1994**, *29*, 203–220. [CrossRef]

42. Beletsky, D.; Schwab, D.; McCormick, M. Modeling the 1998–2003 summer circulation and thermal structure in Lake Michigan. *J. Geophys. Res. Ocean.* **2006**, *111*. [CrossRef]

43. Wang, J.; Hu, H.G.; Schwab, D.; Leshkevich, G.; Beletsky, D.; Hawley, N.; Clites, A. Development of the Great Lakes Ice-circulation Model (GLIM): Application to Lake Erie in 2003-2004. *J. Great Lakes Res.* **2010**, *36*, 425–436. [CrossRef]

44. Huang, A.N.; Rao, Y.R.; Lu, Y.Y.; Zhao, J. Hydrodynamic modeling of Lake Ontario: An intercomparison of three models. *J. Geophys. Res. Ocean.* **2010**, 115. [CrossRef]

45. Fujisaki, A.; Wang, J.; Hu, H.G.; Schwab, D.J.; Hawley, N.; Rao, Y.R. A modeling study of ice-water processes for Lake Erie applying coupled ice-circulation models. *J. Great Lakes Res.* **2012**, *38*, 585–599. [CrossRef]

46. Mellor, G.L.; Yamada, T. Development of a Turbulence Closure-Model for Geophysical Fluid Problems. *Rev. Geophys.* **1982**, *20*, 851–875. [CrossRef]

47. Smagorinsky, J. General circulation experiments with the primitive equations. *Month. Weath. Rev.* **1963**, *91*, 99–164. [CrossRef]

48. Xue, P.F.; Chen, C.S.; Ding, P.X.; Beardsley, R.C.; Lin, H.C.; Ge, J.Z.; Kong, Y.Z. Saltwater intrusion into the Changjiang River: A model-guided mechanism study. *J. Geophys. Res. Ocean.* **2009**, 114. [CrossRef]

49. Schwab, D.J.; Beletsky, D.; DePinto, J.; Dolan, D.M. A hydrodynamic approach to modeling phosphorus distribution in Lake Erie. *J. Great Lakes Res.* **2009**, *35*, 50–60. [CrossRef]

50. Lean, D.R.S.; Knowles, R. Nitrogen Transformations in Lake-Ontario. *Can. J. Fish. Aqua. Sci.* **1987**, *44*, 2133–2143. [CrossRef]

51. Johengen, T.H.; Johannsson, O.E.; Pernie, G.L.; Millard, E.S. Temporal and Seasonal Trends in Nutrient Dynamics and Biomass Measures in Lakes Michigan and Ontario in Response to Phosphorus Control. *Can. J. Fish. Aqua. Sci.* **1994**, *51*, 2570–2578. [CrossRef]

52. Winter, J.G.; Howell, E.T.; Nakamoto, L.K. Trends in nutrients, phytoplankton, and chloride in nearshore waters of Lake Ontario: Synchrony and relationships with physical conditions. *J. Great Lakes Res.* **2012**, *38*, 124–132. [CrossRef]

53. Rodgers, G.K. Time of Onset of Full Thermal Stratification in Lake-Ontario in Relation to Lake Temperatures in Winter. *Can. J. Fish. Aqua. Sci.* **1987**, *44*, 2225–2229. [CrossRef]

54. Holmes, J.D. *Wind Loading of Structures*, 3rd ed.; CRC Press: Boca Raton, FL, USA, 2015.

55. Jarraud, M. *Guide to Meteorological Instruments and Methods of Observation WMO-No. 8*; World Meteorological Organization: Geneva, Switzerland, 2008.

56. CH2M HILL. *Duffin Creek Water Pollution Control Plant Phosphorus Reduction Action Plan Study Final Report. Prepared for The Regional Municipalities of York and Durham by CH2M HILL*; CH2M HILL Canada Limited: Toronto, ON, Canada, 2018.

57. Tomlinson, L.M.; Auer, M.T.; Bootsma, H.A.; Owens, E.M. The Great Lakes Cladophora Model: Development, testing, and application to Lake Michigan. *J. Great Lakes Res.* **2010**, *36*, 287–297. [CrossRef]

58. Canale, R.P.; Auer, M.T. Ecological Studies and Mathematical Modeling of Cladophora in Lake Huron: 7. Model Verification and System Response. *J. Great Lakes Res.* **1982**, *8*, 134–143. [CrossRef]

59. Targets Task Team. *Recommended phosphorus loading targets for Lake Erie. Annex 4 Obectives and Targets Task Team Final Report to the Nutrients Annex Subcommittee*; U.S. EPA and Environment Canada: Washington, DC, USA.

60. *Durham and York Regions. Duffin Creek Water Pollution Control Plant 2014 Annual Performance Report*; The Regional Municipality of Durham and York: ON, Canada, 2014.

61. Lambert, R.S.; Auer, M.T.; Effler, S.W.; Greene, M.R.; Downer, B.E.; Kuczynski, A. Onondaga to Ontario: Management of bioavailable phosphorus in municipal wastewaters for control of Cladophora. *J. Great Lakes Res.* **2015**, *41*, 1106–1113. [CrossRef]

62. Rowe, M.D.; Anderson, E.J.; Wang, J.; Vanderploeg, H.A. Modeling the effect of invasive quagga mussels on the spring phytoplankton bloom in Lake Michigan. *J. Great Lakes Res.* **2015**, *41*, 49–65. [CrossRef]

63. Rowe, M.D.; Anderson, E.J.; Vanderploeg, H.A.; Pothoven, S.A.; Elgin, A.K.; Wang, J.; Yousef, F. Influence of invasive quagga mussels, phosphorus loads, and climate on spatial and temporal patterns of productivity in Lake Michigan: A biophysical modeling study. *Limnol. Oceanogr.* **2017**, *62*, 2629–2649. [CrossRef]